12-2010

Lateral Blood Flow Velocity Estimation Based on Ultrasound Speckle Size Change With Scan Velocity

Tiantian Xu
University of Nebraska-Lincoln

Gregory R. Bashford
University of Nebraska-Lincoln, gbashford2@unl.edu

Lateral Blood Flow Velocity Estimation Based on Ultrasound Speckle Size Change With Scan Velocity

Tiantian Xu and Gregory R. Bashford, *Senior Member, IEEE*

***Abstract*—Conventional (Doppler-based) blood flow velocity measurement methods using ultrasound are capable of resolving the axial component (i.e., that aligned with the ultrasound propagation direction) of the blood flow velocity vector. However, these methods are incapable of detecting blood flow in the direction normal to the ultrasound beam. In addition, these methods require repeated pulse-echo interrogation at the same spatial location. A new method has been introduced which estimates the lateral component of blood flow within a single image frame using the observation that the speckle pattern corresponding to blood reflectors (typically red blood cells) stretches (i.e., is smeared) if the blood is moving in the same direction as the electronically-controlled transducer line selection in a 2-D image. The situation is analogous to the observed distortion of a subject photographed with a moving camera. The results of previous research showed a linear relationship between the stretch factor (increase in lateral speckle size) and blood flow velocity. However, errors exist in the estimation when used to measure blood flow velocity. In this paper, the relationship between speckle size and blood flow velocity is investigated further with both simulated flow data and measurements from a blood flow phantom. It can be seen that: 1) when the blood flow velocity is much greater than the scan velocity (spatial rate of A-line acquisition), the velocity will be significantly underestimated because of speckle decorrelation caused by quick blood movement out of the ultrasound beam; 2) modeled flow gradients increase the average estimation error from a range between 1.4% and 4.4%, to a range between 4.4% and 6.8%; and 3) estimation performance in a blood flow phantom with both flow gradients and random motion of scatterers increases the average estimation error to between 6.1% and 7.8%. Initial attempts at a multiple-scan strategy for estimating flow by a least-squares model suggest the possibility of increased accuracy using multiple scan velocities.**

I. Introduction

Ultrasound has been widely used as a diagnostic tool in the cardiovascular system. It is known that the distribution of the blood velocities within a vessel contains valuable diagnostic information. Likewise, motion of heart tissue is dependent on the health of cardiac muscle [1]. For example, stroke is a type of cardiovascular disease. It affects the arteries leading to and within the brain. A stroke occurs when a blood vessel that carries oxygen and nutrients to the brain is either blocked by a clot or bursts. In the United States, stroke causes death to more than 143 000 people a year, or about 1 of every 17 deaths. It is the third leading cause of death behind heart disease and cancer. Abnormal blood flow is one of the results of stroke [2]. Thus, accurate measurement of blood flow velocity and tissue motion is useful to clinicians.

The Doppler effect in ultrasound (actually a measurement of phase change) is widely used in ultrasound to measure blood flow. Upon insonification by an ultrasound beam, the echoes scattered by blood carry information about the velocity of blood flow. It is used in most commercial ultrasound machines in which the 1-D blood flow velocity vector projection along the axial dimension of the ultrasound beam is estimated. Kasai *et al.* developed an algorithm to quickly estimate the mean velocity over a larger spatial field of view based on an autocorrelation technique [3], which is now commonly referred to as color flow. A complementary method, referred to as spectral Doppler, is capable of visualizing a velocity distribution at a single (resolution-limited) small region of interest by displaying a spectral plot of the (temporal- and wall-filtered) flow signal [4].

However, Doppler is not able to measure the velocity vector projection along the lateral dimension of the ultrasound beam, because there will be no Doppler frequency shift when the surface of the transducer is aligned parallel to the blood flow. Some researchers have formed alternative estimation algorithms to solve this problem. For example, estimating the transit time across the ultrasound beam was proposed for measuring flow lateral to the acoustic axis. One method described by Newhouse and Reid measures the variance of the Doppler signals returned from lateral flow [5]. The spatial quadrature technique was proposed to estimate lateral motion by employing a modulation in the acoustical field in the lateral direction [6], [7]. Direction and magnitude of local blood speckle pattern displacement using consecutive B-mode images were measured by Trahey *et al.*, to predict lateral flow [8]. A more complete review can be found in references [9] and [10]. These methods require multiple scans, unlike the method in this paper which relies on only one image and estimates speckle size.

In 2001, a patent which one of the present authors (GRB) co-authored suggested a technique of blood flow measurement which takes into account the observed stretching of the speckle pattern when viewed on a scanner whose line order was in the same direction as the moving blood [11]. The patent suggested a transform could be developed by comparing speckle size under conditions of no blood flow

Manuscript received May 18, 2010; accepted September 5, 2010.

The authors are with the Dept. of Biological Systems Engineering, University of Nebraska-Lincoln, Lincoln, NE (e-mail: gbashford2@unl.edu).

Digital Object Identifier 10.1109/TUFFC.2010.1743

$$\mathrm{ACVF}_{XX}(\mathrm{lag}) = \frac{\sum(X(:,1:(\mathrm{width}-\mathrm{lag})) - \bar{X}).\times(X(:,(\mathrm{lag}+1):\mathrm{width}) - \bar{X})}{N} \tag{1}$$

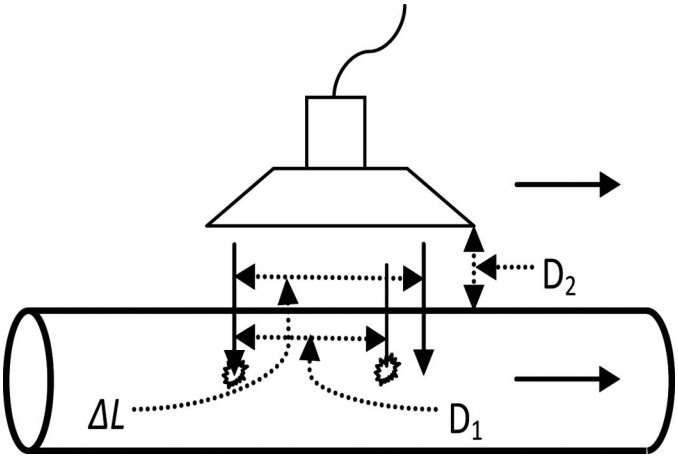

Fig. 1. Scanning geometry when the surface of transducer is parallel to the blood flow.

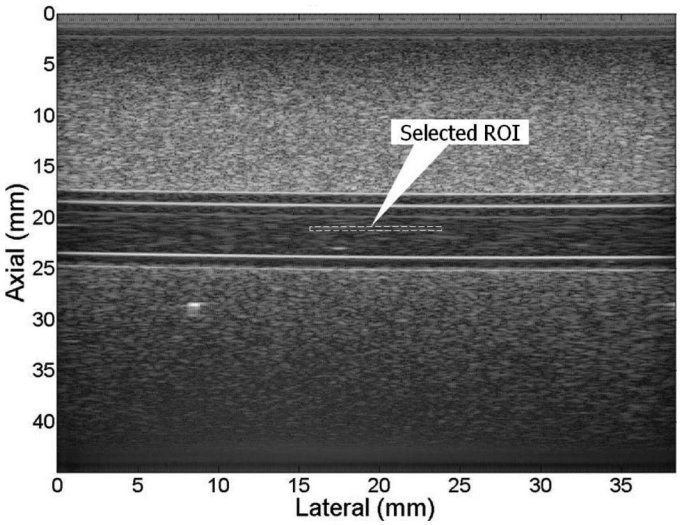

Fig. 2. Region-of-interest (ROI), which is the area in the dashed white line, is selected from every ultrasound B-mode image of the blood flow phantom. It has a width of 50 pixels and height of 20 pixels, corresponding to 6.17 × 0.385 mm.

movement, with-scan movement, and against-scan movement. Such a transform was not developed in the patent.

In our previous studies [12], [13], we call the spatial rate at which individual ultrasound A-lines are collected laterally across the transducer the scan velocity. The scanning geometry is shown in Fig. 1. D_2 is the distance between the surface of the transducer and the vessel. Both scanning and blood flow have the same direction represented by solid arrows. D_1 is the distance traveled by blood flow in one pulse period (both spatial and velocity scales are exaggerated for clarity). The second-order statistics of speckle in ultrasound B-scans was investigated in [14]. In that paper, a speckle size definition was proposed based on the autocovariance function (ACVF) of the speckle. A similar metric for speckle size, namely the full-width at half-maximum (FWHM) of the ACVF of a region-of-interest (ROI) in the ultrasound B-mode image, was used in our previous studies (Fig. 2). It can be estimated by (1), see above, where X is the matrix of an ROI; $\bar{X}$ is the mean value of X; lag is the position shift, which ranges from 0 to the width of the ROI; width is the number of pixels in the lateral dimension; and N is the number of pixels included in the sum operation. As shown in Fig. 2, the ROI is selected from the B-mode image, completely inside an area corresponding to the phantom blood vessel. The axial center of the ROI corresponds to the center of the vessel, and the axial width is chosen with respect to the amount of flow gradient desired in the data. In Fig. 2, a relatively narrow (axially) ROI is chosen, such that the flow gradient is relatively small and thus the flow velocity spectrum relatively narrow. In experiments where a broader flow spectrum is desired (i.e., more flow gradients), a wider (axially) ROI may be chosen.

Depending on the scan sequence direction, speckle corresponding to moving targets or matter will either expand or contract in the direction of motion. Comparing the expanded/compressed size relative to speckle corresponding to stationary targets potentially allows quantitative lateral flow velocity measurement.

Our previous results showed that there is a linear relationship between the reciprocal of the stretch factor and blood flow velocity, which can be represented by

$$\frac{\mathrm{FWHM}-\mathrm{ACVF}_0}{\mathrm{FWHM}-\mathrm{ACVF}_s} = 1 - \frac{V_\mathrm{f}}{V_\mathrm{s}}, \quad \text{when } V_\mathrm{f} < V_\mathrm{s} \tag{2}$$

$$\frac{\mathrm{FWHM}-\mathrm{ACVF}_0}{\mathrm{FWHM}-\mathrm{ACVF}_s} = \frac{V_\mathrm{f}}{V_\mathrm{s}} - 1, \quad \text{when } V_\mathrm{f} > V_\mathrm{s}, \tag{3}$$

where $\mathrm{FWHM}-\mathrm{ACVF}_0$ represents the speckle size of the non-flow condition and $\mathrm{FWHM}-\mathrm{ACVF}_\mathrm{s}$ represents the speckle size of blood flow. Estimation based on this relationship has good performance when the flow velocity is less than the scan velocity. However, when the flow velocity is near or greater than the scan velocity, the estimation error increases significantly. We hypothesize that the main reason for this phenomenon is speckle decorrelation [15]. It could result from either the increasing lag of scan velocity after flow velocity, where the blood flow is moving out of the ultrasound beam, or the flow gradient in the blood flow phantom. Furthermore, only two scanning velocities were used in our previous studies.

The purpose of this paper is to further investigate the relationship between speckle size and blood flow velocity when the blood flow velocity is close to and greater than the scan velocity. This analysis will be done in the lateral dimension only to isolate effects from axial flow. Future studies will address combining axial and lateral motion measurements into 2-D measurement, followed by motion estimation in all three dimensions.

II. Materials and Methods

Both simulated and phantom blood flow data were collected. Data were simulated with and without lateral flow gradients (flow profiles). Four scan velocities were used in each experiment, the details of which follow.

The experimental setup for collecting blood flow data from the blood flow phantom is similar to the one used in our previous studies and is briefly described here. A commercial flow phantom (Optimizer RMI 1425, Gammex, Middleton, WI), was used to simulate blood flow. This phantom contains a tube (5 mm inside diameter, 1.25 mm thickness) through which blood-mimicking fluid is pumped. The fluid has acoustic properties similar to blood (speed of sound 1550 m/s, density 1.03 g/mL). The tube is surrounded by tissue-mimicking material (speed of sound 1540 m/s, attenuation 0.5 dB/cm/MHz).

The V13–5 transducer (192 elements, 6.15 MHz center frequency) of a SONOLINE Antares ultrasound imaging system (Siemens Medical Solutions, Ultrasound Division, Issaquah, WA) was used for data acquisition. The tube is parallel to the surface of transducer, so only lateral flow data were collected. The Axius Direct Ultrasound Research Interface (URI) was employed to transfer ultrasound data (post-beamformation but before any downstream processing) to a computer for further analysis.

The Carotid exam mode was used to scan the flow phantom. The focal depth was 2 cm, the depth at which the tube is located in the phantom. The total imaging depth ranged from 3.5 to 5.5 cm (starting at 0 cm). In each image, 312 lines were collected. The URI includes header information to allow researchers access to key parameters of the experimental setup. The frame rate can be found in the header information. Because 312 lines were collected in each image, the PRF can then be calculated by multiplying the number of lines with the frame rate. The number of lines per centimeter was found to be 81.0 lines/cm. The space interval ΔL between each line can then be calculated as the reciprocal of line density, which is 0.1234 mm. Thus, the scan velocity, that is, the rate at which new ultrasound lines are formed in space, can be derived as:

$$V_{\mathrm{s}} = \Delta L \times \mathrm{PRF}. \tag{4}$$

For each PRF setting, ten B-mode images of the flow phantom with velocity ranging from 0 to 100 cm/s were collected for study, in which the scan direction was the same as the blood flow. Furthermore, ten images of non-flow condition were collected at the same time. In each image, a region of interest (ROI) was selected from the middle of the tube, with an axial length of 20 pixels (0.39 mm) and a lateral length of 50 pixels (6.2 mm), as shown in Fig. 2. This ROI, which is represented as X in (1), was then used to calculate the mean and standard deviation of speckle size. The measured speckle size was used to estimate the flow velocity using (3) and (4).

TABLE I. Parameters of Transducer and Blood Flow Phantom Used in Simulation.

Transducer	
Center frequency	6.15 MHz
Element height	2.5 mm
Element width	0.176 mm
Kerf	25 μm
Number of elements	192
Focal depth	20 mm
Sampling frequency	40 MHz
Blood flow phantom	
Speed of sound	1550 m/s
Depth of tube	20 mm
Diameter of tube	5 mm
Flow direction	Parallel to the surface of the transducer

As observed in our previous studies, the estimation error increases significantly when the flow velocity is near or greater than the scan velocity. We hypothesized that this phenomenon could result from speckle decorrelation caused by the flow gradient in the blood flow phantom. To investigate the effects of flow gradient on speckle size estimation, we used the Field II simulation [16], [17] to simulate blood flow data with and without a flow gradient.

Two flow conditions were simulated: the first had a parabolic velocity distribution in the flow which produces a similar lateral gradient to the flow velocity in the blood flow phantom. The second condition had a constant flow velocity distribution throughout the tube, simulating plug flow. The parameters of the ultrasound transducer and blood flow phantom were set the same as the commercial machine used in blood flow phantom data collection (see Table I).

From the results of our previous studies, we also hypothesized that different scan velocities will have effects on estimation performance. Generally, when the difference between scan velocity and blood flow velocity becomes large, the possibility of speckle decorrelation increases significantly because the blood flow moves out of the ultrasound beam more quickly. Thus, four PRFs (1492, 3241, 4862, and 6483 Hz), corresponding to four different scan velocities, were used in our experiment. For flow velocities ranging from 0 to 100 cm/s, data were collected using four different scan velocities. Our previous studies showed that the estimation performance varies according to scan velocity. Thus, potentially there is an optimal estimation incorporating different scan velocities. One of the ways to do this is to assign weighting coefficients to the velocity estimations made by different scan velocities.

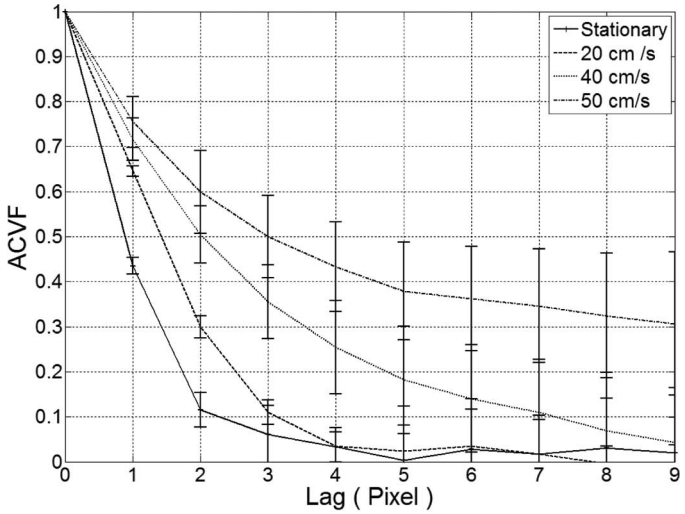

Fig. 3. Autocovariance function (ACVF) of blood flow phantom (scan velocity = 64.8 cm/s). (a) Scan velocity is greater than the blood flow velocity; (b) scan velocity is less than the blood flow velocity. Error bars show ± one standard deviation.

A general least-squares method was used to model this optimal solution [18], which can be represented by

$$\mathrm{EV} \times W = V \tag{5}$$

where EV represents the matrix of estimated velocities; each column contains different estimated results for the blood flow phantom ranging from 0 to 100 cm/s by a certain scan velocity. Because four scan velocities were used in our experiment, the matrix EV contains four columns, thus, its dimension is 10 × 4. The vector V represents actual velocities set to the blood flow phantom, which is a 10 × 1 vector. W is the vector of weighting coefficients we are seeking during the least-square modeling. It is a 4 × 1 vector where each element represents the weighting of estimation by each scan velocity. This least-square model finds the matrix W that minimizes the estimation error $||V - \mathrm{EV} \times W||$.

III. Results

The stretch effect of the speckle between a non-flow condition and flow conditions is shown in Fig. 3. From the graph, it can be seen that the speckle pattern of moving blood-mimicking material is stretched significantly compared with the non-flow condition. Furthermore, the stretch factor decreases as the absolute difference between flow velocity and scan velocity increases.

The relationship between the reciprocal of stretch factor and flow velocity indicated by (2) and (3) is plotted in Fig. 4, Fig. 5, and Fig. 6. To investigate the effects of flow gradient on speckle size estimation, we started with simulation data in which the flow velocity is constant over the whole tube. The results are shown in Fig. 4. It can be seen that the experimental data fit well to the theoretical lines when there is no velocity gradient in the flow. From Fig. 4(a), when the flow velocity exceeds 40 cm/s, the experimental reciprocal stretch factor deviates from theoretical values and stays between 1.3 and 1.5 for the remaining flow velocities.

Fig. 5 shows the relationship between stretch factor and simulated blood flow velocity when the simulated data include flow gradients. Compared with the results in which there is no flow gradient in the tube, the deviation of experimental and theoretical values is more significant. The errors still exist when the scanning velocity is low, which can be seen in Fig. 5(a). Moreover, in Figs. 5(b) and 5(d), the reciprocal of stretch factors are overestimated compared with theoretical values when the flow velocity is less than the scan velocity.

Results of the blood flow phantom data are shown in Fig. 6. Compared with simulated data, the estimation errors are more significant for all four scan velocities. Specifically, the overestimation phenomenon is worse than results from Fig. 5. This can be seen in Fig. 6(b) when the flow velocity is greater than the scan velocity, and in Figs. 6(c) and 6(d), the reciprocal of the stretch factor is always overestimated regardless of whether the flow velocity is greater or less than the scan velocity.

To see the performance of velocity estimation using speckle size more directly, the estimated velocities were plotted versus actual velocities in Fig. 7. Results in three conditions were shown here. In each condition, the estimation results with standard deviation from four different scan velocities were plotted along with the reference line.

Some initial results of the least-squares model are produced using the estimated results from both simulated data and phantom data. The weighting vector is $W_1 = \{0.2, -0.24, 0.2, 0.91\}$ from the simulated data without a flow gradient, and $W_2 = \{-0.36, 0.61, 0.95, -0.26\}$ from the simulated data with a flow gradient. When the phantom data were used, the weighting vector is $W_3 = \{0.52, 0.43, -0.09, 0.26\}$. Using these weighting parameters, the multi-PRF estimation results are calculated by (5) and plotted in Fig. 8.

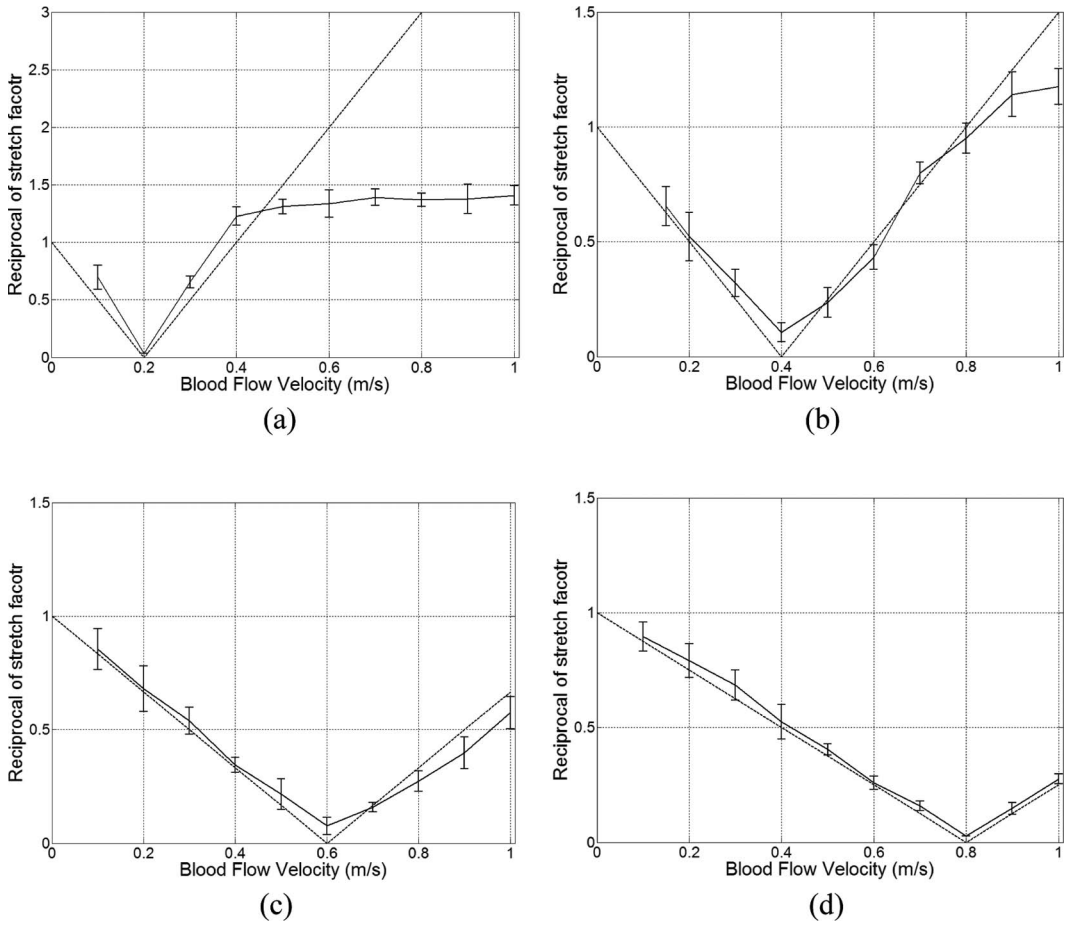

Fig. 4. Reciprocal of stretch factor with standard deviation (without flow gradient). Dashed lines are theoretical lines represented by (2) and (3). (a) Scan velocity is 20 cm/s, (b) scan velocity is 40 cm/s, (c) Scan velocity is 60 cm/s, (d) scan velocity is 80 cm/s.

IV. Discussion

The results in Figs. 4–6 show that there is an approximately linear relationship between the reciprocal of the stretch factor and flow velocity, as seen in (2) and (3). Generally, when there is no gradient in the flow, the experimental results fit the theoretical line well. Furthermore, experimental results from simulated data fit the theoretical line better than the phantom data.

From Figs. 4(a), 5(a), and 6(a), it can be seen that the reciprocal of the stretch factors tend to remain constant around 1.3 to 1.5 in the simulated data and 2 to 2.5 in the blood flow phantom data. The reason for this phenomenon is that in simulated data, the speckle size of the non-flow condition was less than one correlation lag (about 0.7 lags by linear interpolation), which corresponds to one interval between every A-line. When the flow velocity is much faster than the scan velocity, the scatterers leave the interrogation beam in one frame quickly, leading to rapid decorrelation. However, as the speckle pattern in one frame becomes more random, its speckle size will stop decreasing (it does not become any more random) when it approaches a minimum value. In the simulated data, the minimum speckle size of blood flow is 0.5 lags, which gives a maximum reciprocal stretch factor of 1.4. In the data from the flow phantom, the speckle size of the non-flow condition was about 1.2 lags, and the minimum speckle size of flow was 0.5 lags, which gives a maximum reciprocal stretch factor of 2.4.

In Fig 5, when the scan velocity is 40 and 80 cm/s, compared with the results where the flow data do not have a flow gradient, the reciprocal of the stretch factor tends to be overestimated compared with the theoretical values when the flow velocity is less than the scan velocity, which means the speckle size is underestimated in this condition. This phenomenon can be explained by speckle decorrelation caused by the flow gradient. A flow gradient causes scatterers to move relative to one another, which will change their phase relationship. As a result, the speckle pattern in the reflected ultrasound signal will decorrelate, which will produce a smaller speckle size compared with the non-flow gradient condition.

In Fig. 6, where the data are from the blood flow phantom, the decorrelation effects are even more significant than the simulated data. One of the reasons should be the same as for the results from Fig. 5, because the flow gradient exists in the flow phantom. Another reason for the increased decorrelation phenomenon could be inherent random movement of scatterers in the flow phantom. During the simulation, the scatterers did not move in the

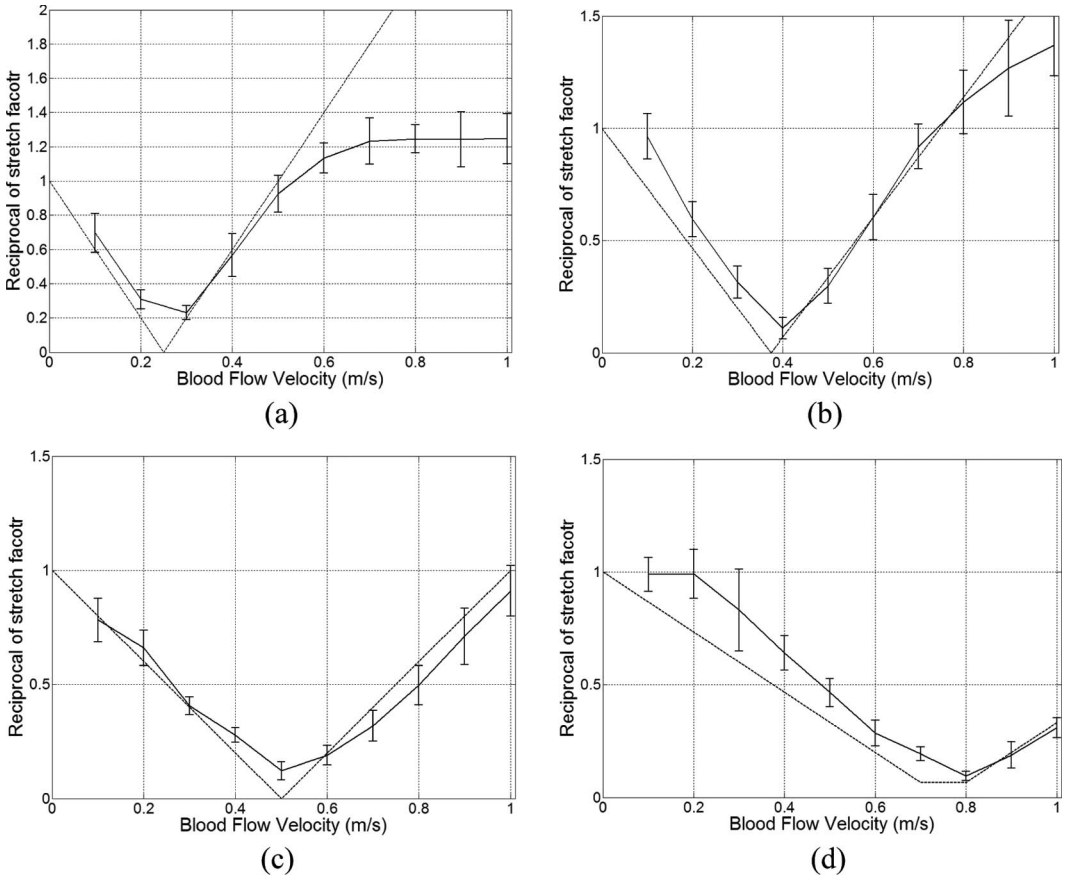

Fig. 5. Reciprocal of stretch factor with standard deviation (with flow gradient). Dashed lines are theoretical lines represented by (2) and (3). (a) Scan velocity is 25 cm/s, (b) scan velocity is 37.4 cm/s, (c) scan velocity is 50 cm/s, (d) scan velocity is 75 cm/s.

TABLE II. The Mean and Standard Deviation of Estimation Error.

Simulated data without flow gradient				
Scan velocity (cm/s)	20	40	60	80
Mean error (% of actual)	81.3	4.4	3.2	1.4
SD of error (% of actual)	98.3	12.3	5.1	3.0
Simulated data with flow gradient				
Scan velocity (cm/s)	25	37.4	50	75
Mean error (% of actual)	51.8	6.8	4.4	4.9
SD of error (% of actual)	62.8	10.4	5.6	8.4
Blood flow phantom data				
Scan velocity (cm/s)	20	40	60	80
Mean error (% of actual)	22.9	6.1	7.2	7.8
SD of error (% of actual)	35.9	8.9	9.2	8.9

axial or elevation dimensions, whereas there is expected to be some random motion of the scatterers within the phantom.

The estimated velocities versus actual simulated and blood flow phantom velocities are plotted in Fig. 7. When the scan velocity is 20 cm/s, the estimation results follow the theoretical line well up to about 50 cm/s flow velocity, then deviate from the actual value with increasing flow velocity. The reason is the same as for the errors of the stretch factor reciprocal when the scan velocity is 20 cm/s. When the scan velocity is 40, 60, and 80 cm/s, the estimation results generally fit the reference line within the range of one standard deviation. To quantitatively evaluate the performance of estimation using different scan velocities, the mean value of estimation errors and standard deviation compared with the reference line is calculated and shown in Table II.

All of the estimation error means are negative; this can be explained by speckle decorrelation, which decreases the speckle size. The largest estimation error mean and standard deviation occurs when the scan velocity is the lowest in simulated data with and without a flow gradient. This is because the scatterer pattern rapidly decorrelates when the flow velocity is much faster than the scan velocity. The overall mean value of estimation error is around 5%, where the maximum error is 7.8% and the minimum is

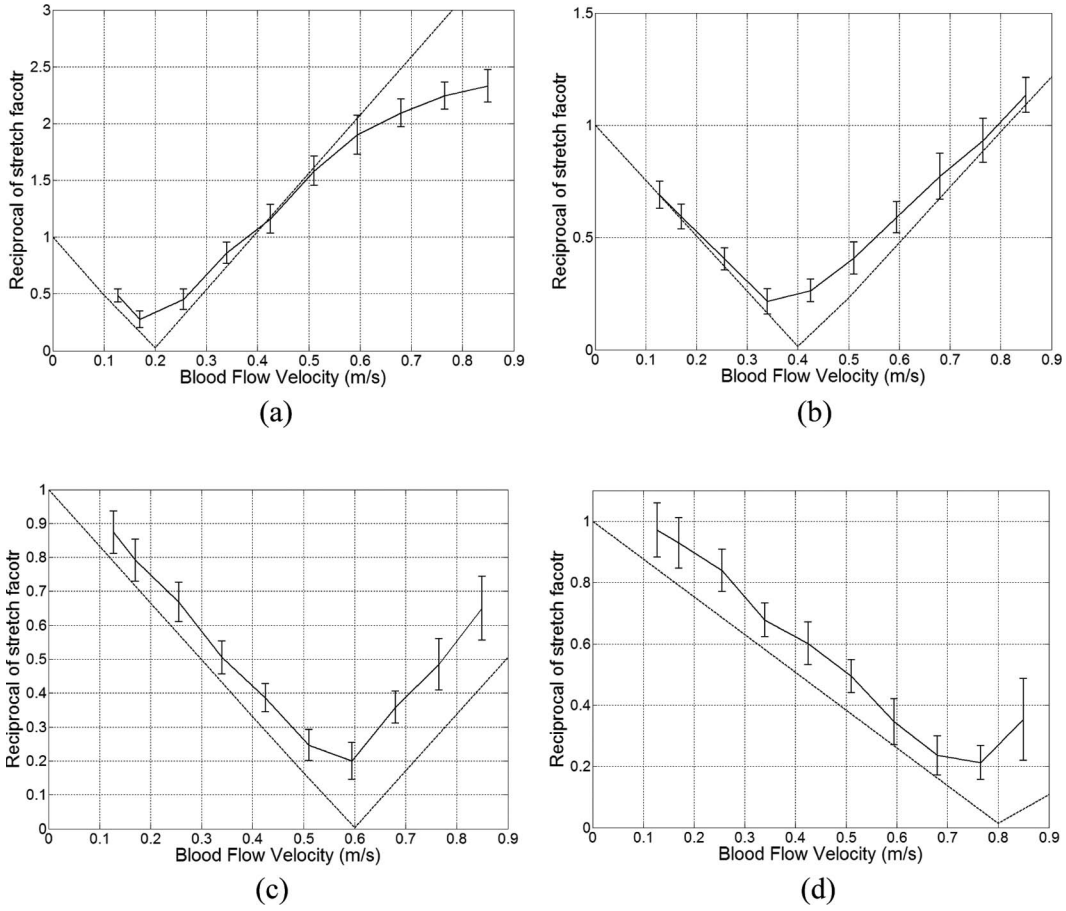

Fig. 6. Reciprocal of stretch factor with standard deviation (blood flow phantom). Dashed lines are theoretical lines represented by (2) and (3). (a) Scan velocity is 20 cm/s, (b) scan velocity is 40 cm/s, (c) scan velocity is 60 cm/s, (d) scan velocity is 80 cm/s.

TABLE III. The Mean of Estimation Errors of Multi-PRF Estimation.

	Simulation		Phantom data
	with flow gradient	without flow gradient	
Mean error (% of actual)	2.9	0.4	1.5

1.4%. Separately, when there is no flow gradient, the average estimation error is between 1.4% and 4.4%. However, when flow gradients are present, the average estimation error increased to between 4.4% and 6.8%, which means that speckle decorrelation caused by flow gradients increased the estimation error. The estimation performance was further degraded in the flow phantom data, where the average estimation error is between 6.1% and 7.8%. This phenomenon results from speckle decorrelation caused by the effects both of flow gradient and relative movement of scatterers in the blood flow phantom.

For the simulated data with a flow gradient, the weighting vector has the largest value when the scan velocity is 50 cm/s and lowest value (actually negative) when the scan velocity is 25 cm/s. This is in accordance with the estimation performance, which can be seen in Fig. 7(b). However, the initial weighting vector for the simulated data without flow gradient gives lowest weighting to the estimation when the scan velocity is 40 cm/s and highest weighting to the estimation when the scan velocity is 80 cm/s. In contrast, the weighting vector for the blood flow phantom has the largest value when the scan velocity is 20 cm/s and lowest value when the scan velocity is 60 cm/s. These results are mainly based on algorithm optimization, and are difficult to be intuitively associated with the estimation results shown in Fig. 7. A particularly interesting result is that some scan speeds are positively weighted whereas others can be negatively weighted. However, it suggests the possibility of making a more accurate estimation with multiple scan velocities. The mean value of multi-PRF estimation errors compared with the reference line is also calculated and shown in Table III. It can be seen that the estimation using multi-PRF significantly reduced the estimation error, which produced much more accurate estimations.

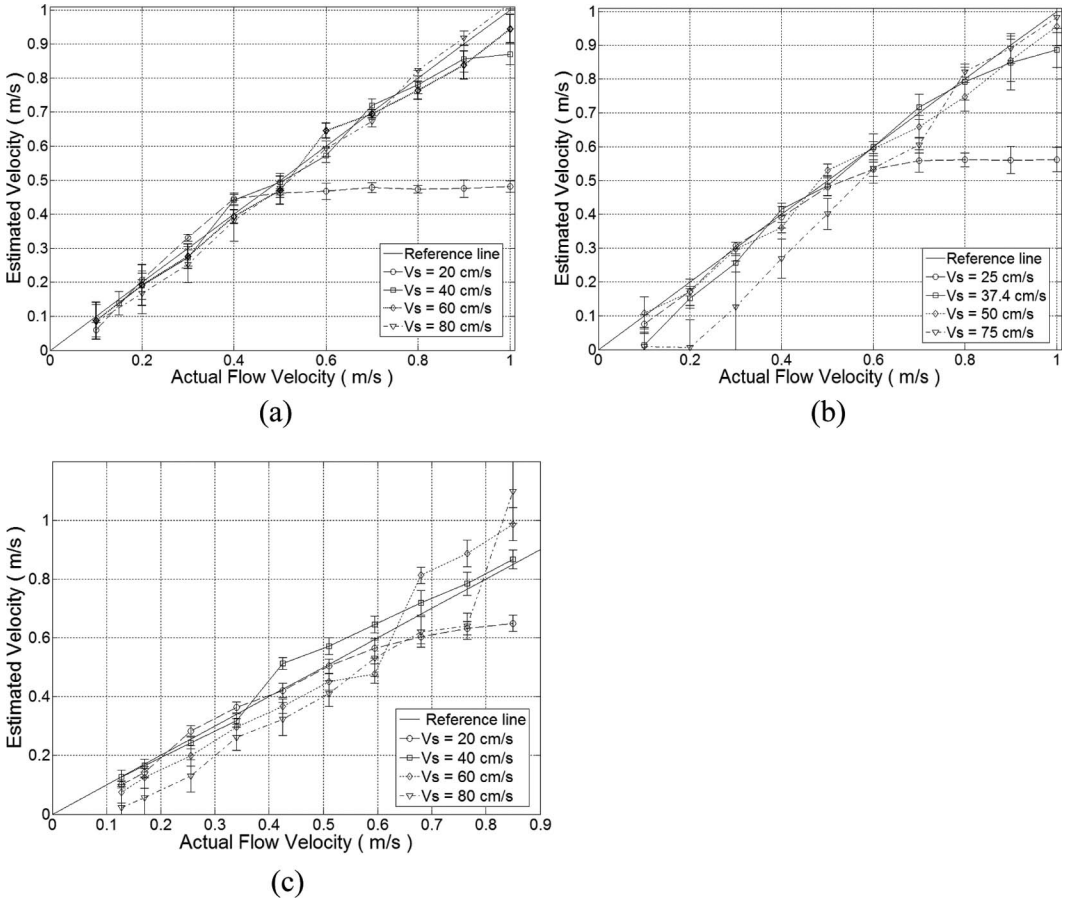

Fig. 7. Estimated velocities versus actual velocities. (a) Simulated data without flow gradient, (b) simulated data with flow gradient, (c) blood flow phantom data.

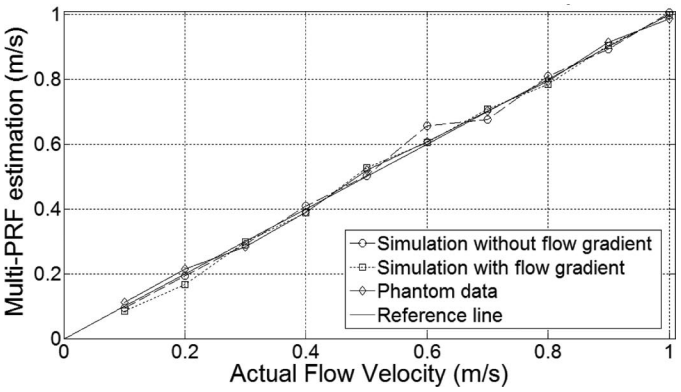

Fig. 8. Multi-PRF estimated velocities versus actual velocities.

V. Conclusion

This paper investigated the relationship between speckle size and (simulated or blood-mimicking) flow velocity during conventional B-mode acquisition. Our previous study developed a linear relationship between the reciprocal of stretch factor and flow velocities. In this paper, the results quantified estimation performance degradation when speckle decorrelation occurred, whether by shear gradients or rate of scatterer movement out of the ultrasound beam. Initial attempts at a multiple-scan strategy for estimating flow using a least-squares model suggest the possibility of increased accuracy by taking into account more than one frame of data. Future studies will focus on the effect of resolution on estimation performance, different transducer geometries (i.e., curved), and the performance under more varied flow conditions (e.g., higher gradients and turbulence).

References

[1] I. A. Hein and W. D. O'Brien Jr., "Current time-domain methods for assessing tissue motion by analysis from reflected ultrasound echoes—A review," *IEEE Trans. Ultrason. Ferroelectr. Freq. Control*, vol. 40, no. 2, pp. 84–102, Mar. 1993.

[2] American Stroke Association, (2010, Apr. 23) *About Stroke*, [Online]. Available: http://www.strokeassociation.org/STROKEORG/AboutStroke/About-Stroke_UCM_308529_SubHomePage.jsp

[3] C. Kasai, K. Namekawa, A. Koyano, and R. Omoto, "Real-time two-dimensional blood flow imaging using an autocorrelation technique," *IEEE Trans. Sonics Ultrason.*, vol. 32, pp. 458–463, 1985.

[4] J. A. Jensen, *Estimation of Blood Velocities Using Ultrasound: A Signal Processing Approach*. Cambridge, UK: Cambridge University Press, 1996.

[5] V. L. Newhouse and J. Reid, "Invariance of Doppler bandwidth with flow axis displacement," in *Proc. IEEE 1990 Ultrasonics Symp.*, vol. 2, pp. 1533–1536.

[6] M. E. Anderson, "Multi-dimensional velocity estimation with ultrasound using spatial quadrature," *IEEE Trans. Ultrason. Ferroelectr. Freq. Control*, vol. 45, no. 3, pp. 852–861, May 1998.

[7] J. A. Jensen and P. Munk, "A new method for estimation of velocity vectors," *IEEE Trans. Ultrason. Ferroelectr. Freq. Control*, vol. 45, no. 3, pp. 837–851, May 1998.
[8] G. E. Trahey, J. W. Allison, and O. T. von Ramm, "Angle independent ultrasonic detection of blood flow," *IEEE Trans. Biomed. Eng.*, vol. BME-34, no. 12, pp. 965–967, 1987.
[9] J. A. Jensen, "Medical ultrasound imaging," *Prog. Biophys. Mol. Biol.*, vol. 93, no. 1–3, pp. 153–165, 2007.
[10] M. F. Insana, "Ultrasonic imaging," in *Wiley Encyclopedia of Biomedical Engineering*, M. Akay, Ed., Hoboken, NJ: Wiley, 2006.
[11] D. J. Hamilton, L. Y. L. Mo, and G. R. Bashford, "Ultrasound based quantitative motion measurement using speckle size estimation," U.S. Patent 6 318 179 B1, Nov. 20, 2001.
[12] T. Xu and G. R. Bashford, "Resolving the lateral component of blood flow velocity based on ultrasound speckle size change with scan direction and speed," in Proc. Annu. Int. Conf. IEEE Engineering in Medicine and Biology Society, vol. 3–6, Sep. 2009, pp. 491–494.
[13] T. Xu and G. R. Bashford, "Further progress on lateral flow estimation using speckle size variation," in *Proc. 2009 IEEE Int. Ultrasonics Symp.*, pp.1383–1386.
[14] R. F. Wagner, S. W. Smith, J. M. Sandrik, and H. Lopez, "Statistics of speckle in ultrasound B-scans," *IEEE Trans. Sonics Ultrason.*, vol. 30, no. 3, pp. 156–163, 1983.
[15] B. H. Friemel, L. N. Bohs, K. R. Nightingale, and G. E. Trahey, "Speckle decorrelation due to two-dimensional flow gradients," *IEEE Trans. Ultrason. Ferroelectr. Freq. Control*, vol. 45, no. 2, pp. 317–327, 1998.
[16] J. A. Jensen and N. B. Svendsen, "Calculation of pressure fields from arbitrarily shaped, apodized, and excited ultrasound transducers," *IEEE Trans. Ultrason. Ferroelectr. Freq. Control*, vol. 39, pp. 262–267, 1992.
[17] J. A. Jensen, "Field: A program for simulating ultrasound systems," *Med. Biol. Eng. Comput.*, vol. 34, suppl. 1, pt. 1, pp. 351–353, 1996.
[18] C. D. Lay, *Linear Algebra and its Applications*, 3rd ed. Reading, MA: Addison-Wesley, 2005.

Tiantian Xu received the B.S. degree in biomedical engineering from the Huazhong University of Science and Technology, Wuhan, P.R. China, in 2007. He is currently working as a Ph.D. student in the Department of Biological Systems Engineering at the University of Nebraska. His current research focuses on new methods of blood flow measurement, including feature tracking and speckle size estimation.

Gregory R. Bashford (M'96–SM'03) received the B.S. degree in electrical engineering from the University of Nebraska, Lincoln, NE, in 1991 and the Ph.D. degree in biomedical engineering from Duke University, Durham, NC, in 1995. He was previously an Image Analysis Engineer at Acuson Corporation, Mountain View, CA; Systems Engineer at GE Medical Systems, Milwaukee, WI; and Senior Scientist at LI-COR Biosciences, Lincoln, NE. In 2003, he joined the faculty of the Biological Systems Engineering department at the University of Nebraska. His research interests include methods and applications of biological and biomedical signal and image analyses.